Journal of Power Sources 203 (2012) 302–307

Contents lists available at SciVerse ScienceDirect

Journal of Power Sources

journal homepage: www.elsevier.com/locate/jpowsour

Short communication

Quasi-Solid-State Dye-Sensitized Solar Cells made with poly(3,4-ethylenedioxythiophene)-functionalized counter-electrodes

Nikolaos Balis [a], Theodoros Makris [a], Vassilios Dracopoulos [b], Thomas Stergiopoulos [c], Panagiotis Lianos [a,b,*]

[a] Engineering Science Dept., University of Patras, 26500 Patras, Greece
[b] Foundation of Research and Technology Hellas-Institute of Chemical Engineering and High Temperature Chemical Processes (FORTH/ICE-HT), P.O. Box 1414, 26504 Patras, Greece
[c] Institute of Physical Chemistry, NCSR Demokritos, 15310 Aghia Paraskevi, Attiki, Greece

ARTICLE INFO

Article history:
Received 17 October 2011
Received in revised form 7 December 2011
Accepted 9 December 2011
Available online 17 December 2011

Keywords:
Dye-Sensitized Solar Cell
PEDOT
Gel electrolyte
Ureasil

ABSTRACT

The present work studies the possibility of substituting Pt by a nanostructured polymer conductor as electrocatalyst on the cathode (counter) electrode of a solar cell. Quasi-Solid-State Dye-Sensitized Solar Cells based on a nanocomposite organic–inorganic Ureasil gel electrolyte were constructed by using either Pt or poly(3,4-ethylenedioxythiophene) (PEDOT)-functionalized counter electrodes. PEDOT gave cells with efficiency only 15% inferior to that reached with Pt cathode electrocatalyst. Therefore, PEDOT is a potential substituent of Pt. PEDOT is not stable in liquid electrolytes but demonstrated good stability in the gel electrolyte presently used. The efficiency of the cell could be further enhanced by placing a mesoporous oxide below the PEDOT layer, which increases the active interfacial area, but this gave cells with limited stability. Materials were characterized by microscopy, UV–Vis spectroscopy and electrochemical techniques.

1. Introduction

The standard configuration for a Dye-Sensitized Solar Cell (DSSC) and for most photoelectrochemical solar cells involves a photoanode electrode, carrying an oxide semiconductor photocatalyst and a photosensitizer, a cathode (counter) electrode, carrying an electrocatalyst, and an electrolyte. The two electrodes are connected through an external circuit, which allows photogenerated electrons to move from the photoanode to the cathode. Internal ionic conductivity is established in the presence of a redox electrolyte, typically I^-/I_3^-. The electrocatalyst is absolutely necessary in order to facilitate electron transfer from the electrode to the electrolyte. The best electrocatalyst is nanoparticulate Pt. There are a number of reasons for Pt superiority. Pt is among the metals with the highest electron work function, it can be easily deposited in nanoparticulate form making the smallest nanoparticles [1,2] and it can adsorb the redox intermediates facilitating electron transfer. However, Pt is scarce and expensive. In addition, it is frequently accused of migration, aggregation and deactivation by poisoning [3]. This matter is a main issue in fuel cells, where the necessary quantity of Pt per unit of electrode surface is higher than in DSSCs. Furthermore, stable attachment of Pt on transparent electrodes necessitates heating at high temperature. This is not possible in the case of flexible cells with plastic electrodes. In any case, the scarcity of Pt opens grounds for research on alternative electrocatalysts for all kinds of electrochemical cells. The most obvious substituents of Pt are carbon nanostructures, which have indeed been studied as electrocatalysts in DSSCs [4,5]. However, these materials necessitate the use of thick films, increasing the internal resistance of the cells [6]. In addition, carbonaceous films are opaque and they cannot be used in semi-transparent cells or in cells excited by radiation entering the cell through the cathode. For this reason, research has been focused on further alternative materials. Conductive polymers seem to be very effective for this purpose. The most popular organic-conductor electrocatalysts are polyaniline [7,8], polypyrrole [9,10], poly(3,4-ethylenedioxythiophene) (PEDOT) [6,11–15], poly(3,4-propylenedioxythiophene) (PProDOT) [16], poly(3,3-diethyl-3,4-dihydro-2*H*-thieno-[3,4-b][1,4]dioxepine) (PProDOT-Et_2) [12,17] and the water soluble version of PEDOT, i.e. poly(3,4-ethylenedioxythiophene) poly(styrenesulfonate) (PEDOT:PSS) [18–21]. These materials have proven themselves capable of competing with Pt as electrocatalysts for DSSCs. Research on these materials focuses on the development of easy synthesis procedures and on their deposition as nanostructured thin films with high specific surface area. For example, the reason that researchers employed PProDOT or PProDOT-Et_2 instead of the simpler PEDOT was to make films with higher specific surface area [12,16,17]. In the same spirit, conductive polymers have been mixed with oxide or carbon nanostructures and other additives in order to increase

* Corresponding author at: University of Patras, Engineering Science Dept., 26500 Patras, Greece. Tel.: +30 2610 997513; fax: +30 2610 997803.
E-mail address: lianos@upatras.gr (P. Lianos).

0378-7753/$ – see front matter © 2011 Elsevier B.V. All rights reserved.
doi:10.1016/j.jpowsour.2011.12.021

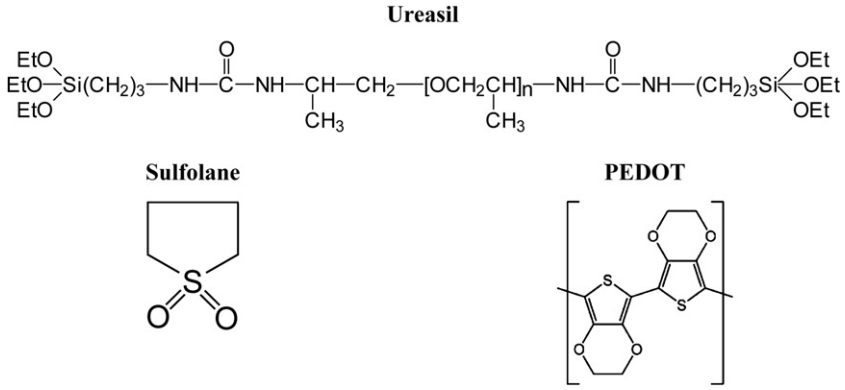

Fig. 1. Chemical structure of the Ureasil precursor, the sulfolane solvent and PEDOT.

roughness and, subsequently, specific surface area [6,8,11,18,21]. In particular, PEDOT:PSS films are very easy to make, for example, by spin coating. These films are smooth and they have relatively low active area. For this reason, cells made with pure PEDOT:PSS counter electrodes gave poor performance with a very low fill factor [18,21]. However, in the presence of agents increasing film roughness, cell efficiency also increased [18,21] making it compatible with cells using Pt-counter electrode. *In brief*, conductive polymer films with sufficiently high specific surface area make counter electrodes for DSSCs compatible with those made with Pt nanoparticles. Organic electrocatalysts give transparent films deposited by easy procedures, which can allow the use of flexible plastic electrodes.

The purpose of the present work is to study the applicability of one of the most important conductive polymer electrocatalysts, i.e. PEDOT, to Quasi-Solid State DSSCs (QSS-DSSC), which are similar to commonly studied DSSCs, but employ a gel electrolyte. In particular, we are interested in gel electrolytes made of nanocomposite organic–inorganic materials based on Ureasil precursors [10,22–29]. The Ureasil precursor used in the present work is depicted in Fig. 1 together with the chemical structure of PEDOT. Condensation of the gel is obtained in the presence of additives including the heterocyclic organic solvent sulfolane, also depicted in Fig. 1. Sulfolane is chosen because of its low volatility (BP 285 °C), its high miscibility with a great variety of solvents and because it improves the structure of the oxide/electrolyte interface. Pure sulfolane has a relatively high melting point (27.5 °C) but usual commercial products are liquid at room temperature. In the present work, it was mixed with 3-methoxy propionitrile to prevent solidification. Cells made with Ureasil gels are easy to construct, since the gel acts as an adhesive holding anode and cathode electrodes together so they require no sealing or encapsulation. Despite the fact that they are practically solid-state devices, they offer relatively high efficiencies, as will be seen below. This relatively high efficiency is reached thanks to the nanocomposite organic–inorganic material, which allows ionic conduction through the organic nano-phase. The gel electrolyte creates a particular environment, different from that offered by liquid electrolytes. For this reason, its compatibility with organic electrocatalysts is worthy of study. In previous work [10], relatively thick and robust polypyrrole films were found to be applicable to such cells. However, thick films were not transparent. In the present work, improved electrodes were made by employing thin transparent PEDOT films.

2. Experimental

2.1. Materials

All materials were from Aldrich unless otherwise specified. Tetraprotonated cis-bis(isothiocyanato)bis(2,2′-bipyridyl-4,4′-dicarboxylato)-ruthenium (II) dye (Ruthenium 535 bis TBA, or N719) was from Solaronix, Switzerland; Commercial nanocrystalline (nc) titania was Degussa P25 and SnO_2:F (FTO) transparent electrodes (resistance 8 Ω sq.$^{-1}$) were purchased from Pilkington, USA.

2.2. Synthesis of the Ureasil precursor

The gel electrolyte was based on the Ureasil precursor shown in Fig. 1. Its synthesis has been reported in a previous publication [30]. Briefly, a Jeffamine, poly(propylene glycol)bis(2-aminopropylether), of molecular weight 230 and 3-isocyanatopropyltriethoxysilane were mixed in tetrahydrofuran (THF) under reflux (64 °C) for 6 h. The molar ratio was 1:2. The isocyanate group of 3-isocyanatopropyltriethoxysilane reacts with the amino groups of poly(propylene glycol)bis(2-aminopropylether) (acylation reaction) producing urea connecting groups between the polymer units and the inorganic part. After evaporation of THF under vacuum, a viscous material is obtained, which is stable at room temperature for several months.

2.3. Synthesis of the Ureasil gel electrolyte containing the redox couple I^-/I_3^-

1.6 g of sulfolane and 0.8 of 3-methoxy propionitrile were mixed under stirring with 0.7 g of the above Ureasil precursor, 0.35 mL of acetic acid (AcOH), 0.12 g LiI and 0.12 g 1-methyl 3-propylimidazolium iodide. When the solution was clear, we added 0.06 g I_2. Thus the molar ratio of I^- to I_2 was approximately 6:1. Finally, we added about 0.5 tert-butylpyridine and 0.1 mol L^{-1} guanidinium thiocyanate, which are known to raise the open-circuit voltage and the short-circuit current in DSSCs, respectively. The sol was stirred for several hours before application. During this period, a slow solvolysis takes place developing silica bonds between precursor chains and leading to condensation and gel formation [30].

2.4. Deposition of nc-TiO_2 and dye adsorption

A FTO glass electrode was cut in the necessary dimensions and was carefully cleaned, first by washing with soap and then by subsequent sonication in isopropanol, water and acetone. Then a densely packed nanocrystalline titania (nc-TiO_2) layer was first deposited on the FTO electrode similarly to a previously published procedure [28]: 3.5 g of the non-ionic surfactant Triton X-100 was mixed with 19 mL ethanol. Then we added 3.4 mL of AcOH and 1.8 mL of titanium tetraisopropoxide under vigorous stirring. After a few minutes stirring, the film was deposited by dipping and then it was left to dry in air for a few minutes. Finally, it was calcined at 550 °C. The temperature ramp was 20 °C min^{-1} up to 550 °C

and the sample was left for about 10 min at that temperature. The procedure was repeated once more. Each layer gave a thin nanostructured film of about 170 nm thickness, as measured by its FE-SEM profile [10]. On the top of this compact nanostructured layer we deposited commercial Degussa P25. For this purpose, a paste of titania P25 was prepared according to Ref. [31]. The paste was applied by doctor blading using 3 M Scotch tape as spacers. It was finally calcined again at the same rate up to 550 °C. The thickness of the film obtained was about 6 μm as measured by its FE-SEM profile [10]. As soon as it was taken out of the oven, it was dipped in acetonitrile:tert-butanol (50:50%, v/v) solution containing 5 mmol L^{-1} of the N719 dye and was left overnight. The film was then heavily colored with adsorbed dye.

2.5. Construction of the counter electrodes

Some counter electrodes were functionalized with Pt, for comparison. For this purpose, a solution of 0.02 mol L^{-1} H_2PtCl_6 in isopropanol [32] was spin-coated on properly cleaned FTO at 2000 rpm. The film obtained was calcined at 450 °C for 15 min. PEDOT counter electrodes were deposited by electrodeposition according to previously published procedures [15,33], using the corresponding monomer 3,4-ethylenedioxylthiophene (EDOT), which polymerized during the process. The process was carried out by employing a three-electrode set up with a Pt sheet as a counter-electrode and Ag/AgCl as a reference electrode. The solvent was acetonitrile containing 0.1 mol L^{-1} $LiClO_4$ and 0.2 mol L^{-1} EDOT. The applied potential was +2 V (vs. Ag/AgCl) for 10 s. Voltage and deposition time was optimized by studying different possibilities; voltage was varied in the range 1.0–2.5 V and time varied between 2 and 15 s. The above chosen values gave optimal results. After electrodeposition, the film was rinsed several times with acetonitrile and dried in a stream of nitrogen. The substrate was a carefully cleaned plain FTO electrode. Alternatively, a thin layer of a nanocrystalline oxide was first deposited on FTO and then PEDOT was electrodeposited under the same as above conditions. Three different oxide layers were tried: (1) a single dense layer of nanocrystalline titania deposited by the same sol–gel procedure as the bottom layer of nc-TiO_2 on the photoanode electrode, described in Section 2.4. The thickness was 170 nm, as above. (2) A nanocrystalline titania layer, deposited by using a paste made of titania P-25, as in Section 2.4. The thickness of this layer was approximately 6 μm, as above. (3) A thin NiO layer, about 250 nm, measured again by FE-SEM. This film was made by modifying a previously published procedure [34]: 360 mg $Ni(OCOCH_3)_2{\cdot}4H_2O$ (nickel acetate tetrahydrate) was dehydrated by heating at 100 °C for 2 h. Then it was mixed with 5 mL of water and stirred overnight. The green precipitate was collected after centrifugation and was mixed with a few drops of ethanol. The paste obtained was applied on the FTO electrode, which was heated up to 400 °C with a temperature ramp of 20 °C min^{-1}.

2.6. Cell construction

Cells were made in the standard configuration. An FTO glass electrode was cut in the necessary dimensions and was carefully cleaned as described in Section 2.4. On this clean electrode we applied the nc-TiO_2 layers and adsorbed the dye-sensitizer N719, as already detailed in Section 2.4. Then the film, colored with the adsorbed dye, was rinsed with acetonitrile, dried in a N_2 stream and heated for a few minutes at 100 °C. The next step was to deposit the Ureasil sol enriched with the additives described in Section 2.3 and the I^-/I_3^- redox couple and to apply the counter electrode. One drop of the sol, prepared as detailed in Section 2.3, was placed on the top of the N719/nc-TiO_2 film. A Pt or PEDOT-functionalized FTO electrode was applied on the top and held together with a metal clip. It was left like this for a few hours. During this time, the sol becomes a solid gel and acts as adhesive resin steadily holding the two electrodes together. Wire connection was made by using auto-adhesive copper ribbons. No encapsulation or sealing of the cell has been done and all measurements were performed under ambient conditions. The actual size of the cell was 1 cm^2 but illumination of the samples was made through a mask allowing for an active area of 0.2 cm^2.

2.7. Measurements

Illumination of the samples was made with a PECCELL PEC-L01 Solar Simulator set at 100 mW cm^{-2}. *I–V* characteristics were recorded under ambient conditions with a Keithley 2601 source meter. Field Emission Scanning Electron Microscope (FE-SEM) images were recorded with a LEO SUPRA 35VP device. Electrochemical impedance spectra (EIS) on symmetrical cells of the type counter electrode/electrolyte/counter electrode were recorded using an Autolab PGSTAT-30 potentiostat, equipped with a frequency response analyzer (FRA), at −0 V vs. the counter-electrode in the dark and recorded over a frequency range of 100 kHz to 10 mHz. Fitting was made by employing the software provided with the instrument, assuming a classical Warburg circuit [35]. A minimum set of 3 measurements were carried out for each cell and mean values of these were taken. Cyclic voltamograms were made by employing a Pt sheet as counter and a Ag/AgCl as reference electrode. The electrolyte contained 0.01 mol L^{-1} LiI, 0.001 mol L^{-1} I_2 and 0.1 mol L^{-1} $LiClO_4$ in acetonitrile [6–9].

3. Results and discussion

3.1. Characterization of the counter electrodes

FTO electrodes were prepared by depositing either Pt or PEDOT, as described in Section 2.5. It is of interest to show images of plain and Pt-functionalized FTO electrodes, which do not usually appear in the literature. The FE-SEM images of the presently used FTO electrodes can be seen in Fig. 2a and b. The FTO layer is approximately 700 nm thick (measured by means of the FE-SEM profile) and it consists of nanoparticles of highly dispersed sizes but packed in an efficient manner thus providing sufficient conductivity. Deposition of Pt, by spin-coating a solution in isopropanol, as described in Section 2.5, created a very thin layer of Pt nanoclusters separated from each other and rather uniformly dispersed (Fig. 2c and d). The thickness of such a film is practically impossible to measure. This type of Pt functionalized FTO gives the best results when applied to DSSCs. In some works, other researchers present Pt films, which are relatively thick and highly concentrated (see, for example, Refs. [12,17]). Such films are unnecessary and harmful. Unnecessary, because much less Pt suffices to do the job and harmful, because the extra Pt screens the rest of the material and decreases electrode transparency.

We have tried various deposition conditions for the PEDOT layer by varying voltage and deposition time. It was concluded that +2 V vs. Ag/AgCl, previously discussed in the literature [15,33], is the best choice for the voltage. The deposition time affected the thickness of the film. Film thickness was approximately measured by its FE-SEM profile. Thus it was found that about 2 s of deposition time gives a film about 50 nm thick. We found that in order to obtain a robust film, it was necessary to apply the above electric bias for 10 s leading to films about 250 nm thick. Thinner films were destroyed during measurements. PEDOT films on FTO glasses are not very stable in a liquid electrolyte. *This fact is unfortunately not much discussed in the literature*. However, in the case of the presently proposed QSS-DSSCs, the solid gel electrolyte does not let the organic conductor

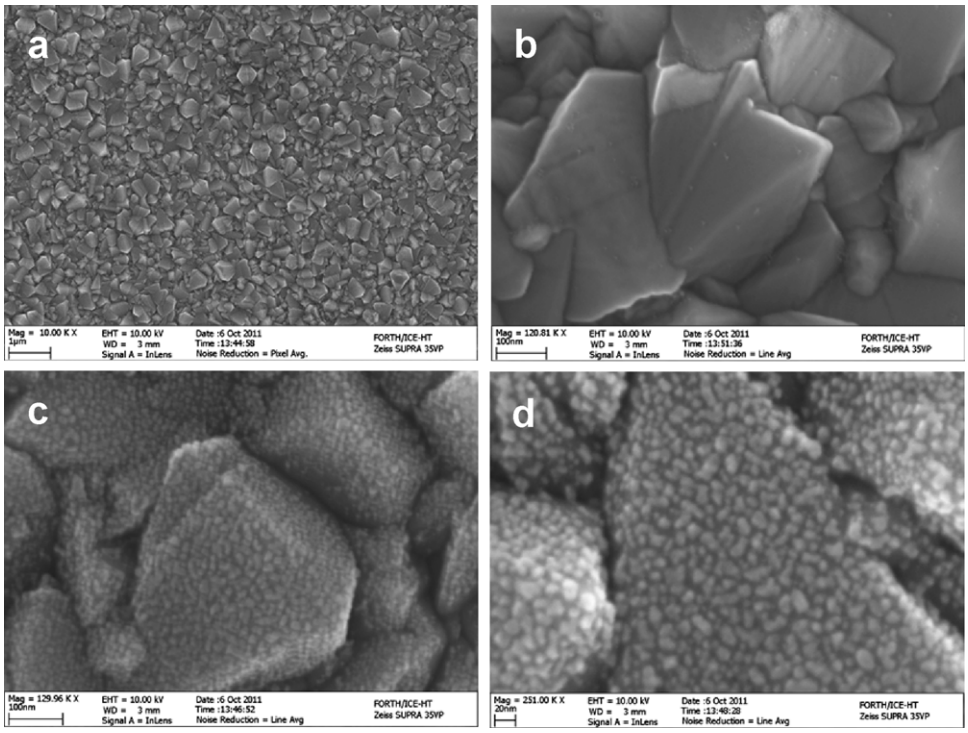

Fig. 2. FE-SEM images of (a) plain FTO electrode at low magnification; (b) plain FTO electrode at high magnification; (c) and (d) Pt/FTO electrodes at two different magnifications. The scale bar is (a) 1 μm; (b) and (c) 100 nm; and (d) 20 nm.

to dissolve in the electrolyte. This is a great advantage provided by the gel electrolyte. We have concluded that the film should not be too thin, even though thicker films affect transparency, because it then loses its coherence. PEDOT film transparency can be judged by examining the UV–vis spectra in Fig. 3. It is seen that light transmittance substantially decreases in going from the thin film (2 s deposition, 50 nm) to the thick film (10 s deposition, 250 nm). Fortunately, the dye sensitizer (N-719), the absorption spectrum of which is also shown in Fig. 3, mainly absorbs light in the spectral region where PEDOT demonstrates higher transmittance. Therefore, the actual PEDOT films employed to make solar cells in the present work were products of 10 s deposition time. The FE-SEM images of the PEDOT films are shown in Fig. 4. The film deposited for 10 s was more compact than the film of 2 s. Both films were nanostructured thus providing high active interface.

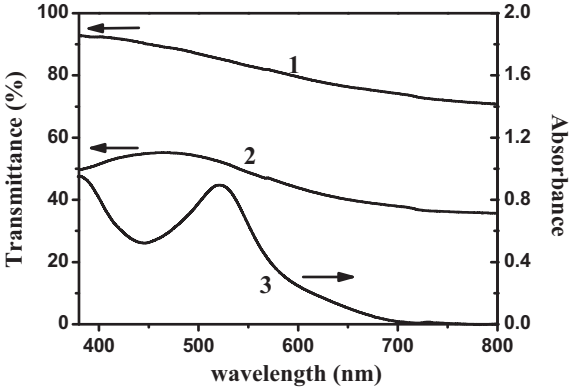

Fig. 3. UV–vis transmittance and absorption spectra: (1) transmittance of PEDOT film deposited for 2 s; (2) transmittance of PEDOT film deposited for 10 s; and (3) absorption spectrum of the dye-sensitizer N-719 in acetonitrile.

The redox activity of the Pt and PEDOT films was demonstrated by cyclic voltametry in an electrolyte that contained the I^-/I_3^- redox couple. The results can be seen in Fig. 5. Curves 1 and 2 contain the oxidation and reduction peaks typically observed with this redox couple. The first anodic peak (+0.30 V for PEDOT and +0.44 V for Pt) corresponds to reaction (1) and the second (+0.78 and +0.88 V) to reaction (2) [6]:

$$3I^- \leftrightarrow I_3^- + 2e^- \quad (1)$$

$$2I_3^- \leftrightarrow 3I_2 + 2e^- \quad (2)$$

The current range of the PEDOT electrode was wider than that of the Pt electrode. This is indicative of the efficiency of the PEDOT electrode. Nevertheless, it must be underlined that the quantity of the active material affects the current range. Thus the current was smaller when the PEDOT films (not shown) were thinner. The above results constitute an additional argument for choosing to use a relatively thick PEDOT film, i.e. deposited for 10 s, obviously capable of reducing sufficient redox species comparable or even more numerous than in the case of Pt itself. Fig. 5 shows a third cyclic voltamogram corresponding to a plain FTO electrode, without any catalytic layer. As expected, a very small current and no redox peaks were detected in this case.

A stricter comparison between Pt and PEDOT catalysts under real (gel) electrolyte conditions was made by EIS measurements (Section 2.7) using symmetrical cells made with the corresponding electrodes and the gel electrolyte used for making the solar cells themselves (Sections 2.3 and 2.6). One cell was made with plain FTO electrodes, for comparison. The results are shown in Fig. 6 and Table 1. Pt and PEDOT curves demonstrated similar behavior. They are composed of one well-defined semicircle attributed to charge transfer at the electrode/electrolyte interface and an additional RC circuit attributed to the Warburg diffusion of ions in the electrolyte, which does not close at the frequencies studied. Plain FTO cells gave only one semicircle, for probably hindered diffusion, due to the

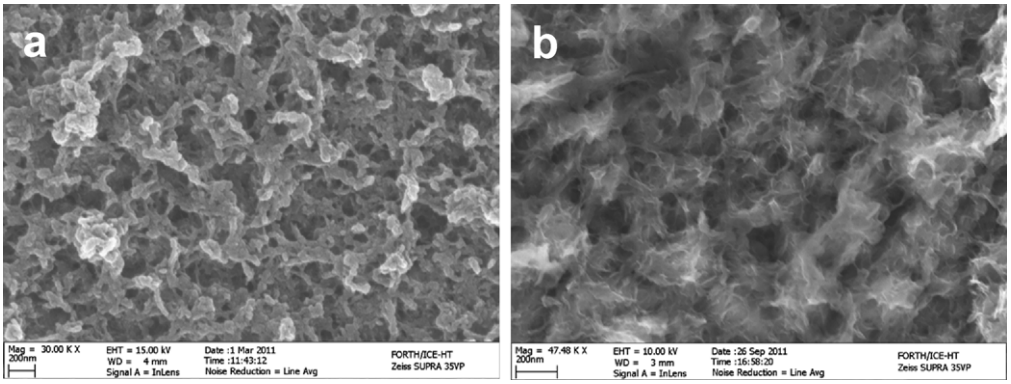

Fig. 4. FE-SEM images of PEDOT films electrodeposited on FTO electrodes for two deposition times: (a) 2 s and (b) 10 s. The scale bar is 200 nm for both images.

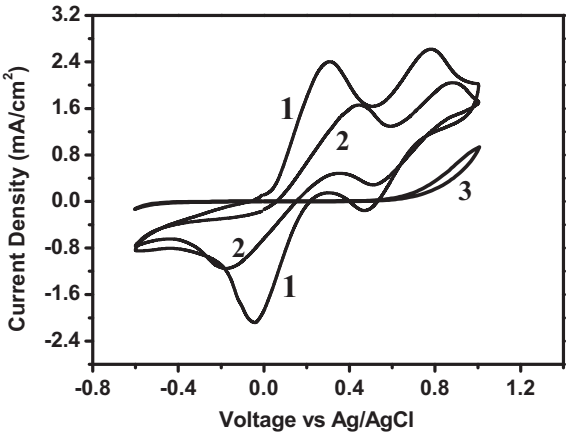

Fig. 5. Cyclic voltamograms for FTO electrodes with deposited PEDOT (1) and Pt (2). Curve (3) corresponds to plain FTO without any catalytic layer. The electrolyte contained 0.01 mol L^{-1} LiI, 0.001 mol L^{-1} I_2 and 0.1 mol L^{-1} $LiClO_4$ in acetonitrile [6–9].

very large interfacial resistance at the electrode/electrolyte interface. This is expected, since I_3^- cannot be easily reduced at the FTO electrode, because of the absence of catalytic nanoparticles (cf. data of Fig. 5). By proper fitting of the EIS diagrams with simple electrical equivalent circuits [36] we could easily determine the values of basic parameters. They were significantly affected by altering the electrode, as seen in Table 1. All cells had similar Ohmic resistance

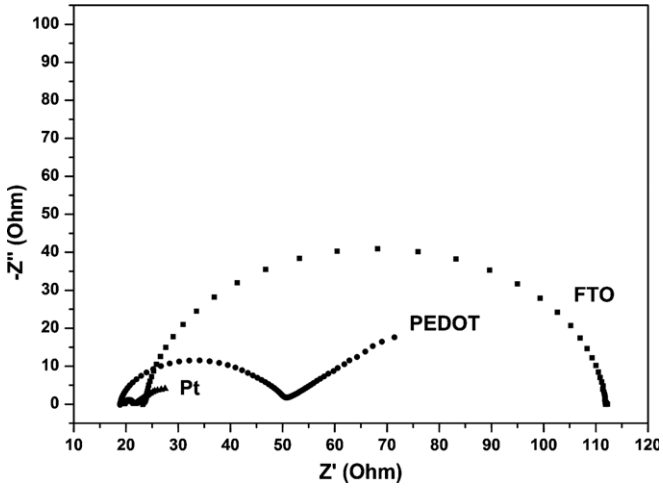

Fig. 6. EIS diagrams for the three symmetrical cells based on plain FTO, PEDOT/FTO and Pt/FTO electrodes.

Table 1
Results of the EIS analysis of the FTO, Pt/FTO and PEDOT/FTO symmetrical cells.

Type of electrode	R_s (Ω)	R_{ct} (Ω)	Y_0 ($\times 10^{-4}$ S)	n	W ($\Omega^{-1/2}$)
FTO	21.80	98.9	0.14	0.95	–
Pt	22.64	2.3	0.68	0.90	0.55
PEDOT	25.18	32.3	0.28	0.84	0.13

R_s is the contact resistance (including the sheet resistances of the two identical electrodes).
R_{ct} stands for the charge transfer resistance at the electrode/electrolyte interface.
Y_0 is a parameter defining the capacitance (Q_{DL}) at the electrode/electrolyte interface through the equation $Y_0 = Q_{DL}\ (j\omega)^n$.
n is a constant ranging from 0 to 1, representing the non ideality of the dependence of the capacitance on the frequency.
W is the Warburg impedance.

(in the range of 21–25 Ω), highlighting the fact that both Pt and PEDOT were well deposited on the FTO electrode forming a good Ohmic contact. However, significant differences were observed on the charge transfer resistances at the electrode/electrolyte interface (R_{ct}). It was then obvious that Pt electrodes operate more effectively than PEDOT electrodes showing significantly smaller values of R_{ct} accompanied with larger values of Y_0. However, the diffusion of ions is easier in the case of the PEDOT electrodes (smaller values of W for the PEDOT electrodes). This is expected, due to the large active interface provided by PEDOT, compared to the limited interface of the Pt layer (cf. Figs. 2 and 4). An improved diffusion of triiodide ions could influence in a positive way the regeneration of iodide at the counter electrode, which, in turn, could affect the regeneration of the sensitizer. Different trends in the values of R_{ct} and W have already been observed on other materials used as counter electrodes in DSSCs, such as mesoporous carbon electrodes [37].

3.2. Cell I–V characteristics

The *I–V* characteristics of the cells made with various counter electrodes are presented in Table 2 and Fig. 7. Pt-functionalized counter-electrodes were the most effective. The efficiency dropped in the case of the PEDOT system and was reduced by about 15% compared to that of Pt. This is a rather small loss and allows PEDOT to be

Table 2
I–V characteristics of the cells made with five different counter electrodes.

Counter electrode	I_{sc} (mA cm^{-2})	V_{oc} (V)	Fill factor	Efficiency (%)
Pt/FTO	15.3	0.67	0.67	6.9
PEDOT/FTO	12.5	0.67	0.70	5.9
PEDOT/thin TiO_2/FTO	14.2	0.67	0.67	6.4
PEDOT/thick TiO_2/FTO	14.5	0.67	0.66	6.4
PEDOT/NiO/FTO	14.9	0.66	0.66	6.5

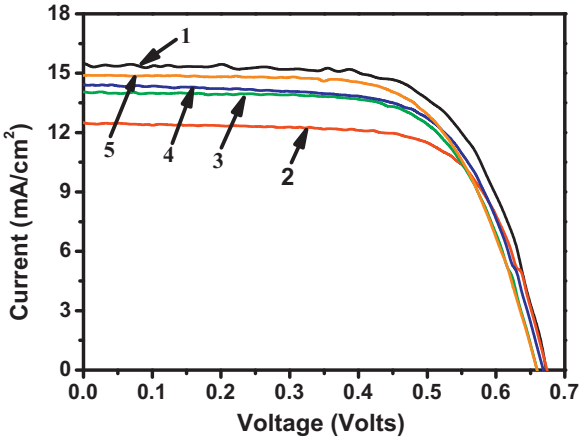

Fig. 7. *I–V* curves for the cells made with the five different counter electrodes: (1) Pt/FTO; (2) PEDOT/FTO; (3) PEDOT/thin TiO_2/FTO; (4) PEDOT/thick TiO_2/FTO; and (5) PEDOT/NiO/FTO.

considered as a valuable substitute of Pt. It is interesting to examine data obtained with counter electrodes bearing a nanocrystalline oxide interlayer between the FTO electrode and the PEDOT layer. These mesoporous oxides were first deposited on FTO, as described in Section 2.5. Then PEDOT was electrodeposited under the same conditions as in the case of plain FTO electrodes. The presence of mesoporous oxides increases the active catalyst/electrode surface and this should have beneficial effects on cell performance. Indeed, as seen in Table 2 and Fig. 7, the efficiency of the cell increased in the presence of such mesoporous oxide interlayers. This is true for fresh samples, but in the course of time, all counter electrodes bearing oxide layers deteriorated and lost all characteristics, i.e. current, voltage and fill factor (data not shown). On the contrary, plain PEDOT/FTO electrodes demonstrated a remarkable stability, once more establishing PEDOT as a valuable substitute of Pt in QSS-DSSCs. At this stage, we have no explanation for the cell failure in the presence of oxide layers other than the possibility of PEDOT oxidation by the mesoporous oxide. This matter needs further study but it is beyond the purpose of the present work.

The efficiency of the above cells, is lower than that observed with liquid electrolyte solar cells (current record about 11% [38]). This is expected, since the ionic conductivity in a solid gel is expected to be much lower than in a liquid electrolyte of the same redox species. Still, the efficiency is satisfactory, taking into account the easiness of cell construction and the fact that it necessitates no sealing or encapsulation.

4. Conclusions

This work describes the construction of a Quasi-Solid-State Dye-Sensitised Solar Cell (QSS-DSSC) based on a Ureasil nanocomposite organic–inorganic gel electrolyte and on a PEDOT/FTO counter electrode. PEDOT is a successful substituent for Pt as electrocatalyst giving a solar cell efficiency only 15% inferior to a cell made with a Pt/FTO counter electrode. The efficiency of the cell could be further enhanced by placing a mesoporous oxide interlayer below PEDOT, which increases the active interface, but this gave cells with limited stability, contrary to the remarkably stable cells made with plain PEDOT/FTO counter electrodes. PEDOT films of various thicknesses were examined and it was found that a PEDOT layer about 250 nm thick provides enough structural coherence to obtain a stable film.

References

[1] Y. Mizukoshi, Y. Makise, T. Shuto, J. Hu, A. Tominaga, S. Shironita, S. Tanabe, Ultrason. Sonochem. 14 (2007) 387.
[2] N. Strataki, N. Boukos, F. Paloukis, S.G. Neophytides, P. Lianos, Photochem. Photobiol. Sci. 8 (2009) 639.
[3] M. Winter, R.J. Brodd, Chem. Rev. 104 (2004) 4245.
[4] T.N. Murakami, S. Ito, Q. Wang, Md.K. Nazeeruddin, T. Bessho, I. Cesar, P. Liska, R. Humphry-Baker, P. Comte, P. Pechy, M. Gratzel, J. Electrochem. Soc. 153 (2006) A2255.
[5] K. Suzuki, M. Yamaguchi, M. Kumagai, S. Yanagida, Chem. Lett. 32 (2003) 28.
[6] K.-M. lee, W.-H. Chiu, H.-Y. Wei, C.-W. Hu, V. Suryanarayanan, W.-F. Hsieh, K.-C. Ho, Thin Solid Films 518 (2010) 1716.
[7] Q. Li, J. Wu, Q. Tang, Z. Lan, P. Li, J. Lin, L. Fan, Electrochem. Commun. 10 (2008) 1299.
[8] H. Sun, Y. Luo, Y. Zhang, D. Li, Z. Yu, K. Li, Q. Meng, J. Phys. Chem. C 114 (2010) 11673.
[9] J. Wu, Q. Li, L. Fan, Z. Lan, P. Li, J. Lin, S. Hao, J. Power Sources 181 (2008) 172.
[10] T. Makris, V. Dracopoulos, T. Stergiopoulos, P. Lianos, Electrochim. Acta 56 (2011) 2004.
[11] Y. Saito, W. Kubo, T. Kitamura, Y. Wada, S. Yanagida, J. Photochem. Photobiol. A: Chem. 164 (2004) 153.
[12] K.-M. Lee, P.-Y. Chen, C.-Y. Hsu, J.-H. Huang, W.-H. Ho, H.-C. Chen, K.-C. Ho, J. Power Sources 188 (2009) 313.
[13] S. Ahmad, J.-H. Yum, Z. Xianxi, M. Gratzel, H.-J. Butt, M.K. Nazeeruddin, J. Mater. Chem. 20 (2010) 1654.
[14] A.J. Mozer, D.K. Panda, S. Gambhir, T.C. Romeo, B. Winther-Jensen, G.G. Wallace, Langmuir 26 (2010) 1452.
[15] H. Tian, Z. Yu, A. Hagfeldt, L. Kloo, L. Sun, J. Am. Chem. Soc. 133 (2011) 9413.
[16] S. Ahmad, J.-H. Yum, H.-J. Butt, M.K. Nazeeruddin, M. Gratzel, Chem. Phys. Chem. 11 (2010) 2814.
[17] K.M. Lee, C.-Y. Hsu, P-Y. Chen, M. Ikegami, T. Miyasaka, K.C. Ho, Phys. Chem. Chem. Phys. 11 (2009) 3375.
[18] J.-G. Chen, H.-Y. Wei, K.-C. Ho, Sol. Energy Mater. Sol. Cells 91 (2007) 1472.
[19] G.D. Sharma, P. Suresh, M.S. Roy, J.A. Mikroyannidis, J. Power Sources 195 (2010) 3011.
[20] T. Muto, M. Ikegami, T. Miyasaka, J. Electrochem. Soc. 157 (2010) B1195.
[21] K. Kitamura, S. Shiratori, Nanotechnology 22 (2011) 195703.
[22] E. Stathatos, P. Lianos, U. Lavrencic-Stangar, B. Orel, Adv. Mater. 14 (2002) 354.
[23] E. Stathatos, P. Lianos, S.M. Zakeeruddin, P. Liska, M. Gratzel, Chem. Mater. 15 (2003) 1825.
[24] E. Stathatos, P. Lianos, A.S. Vuk, B. Orel, Adv. Funct. Mater. 14 (2004) 45.
[25] E. Stathatos, P. Lianos, V. Jovanovski, B. Orel, J. Photochem. Photobiol. A: Chem. 169 (2005) 57.
[26] V. Jovanovski, E. Stathatos, B. Orel, P. Lianos, Thin Solid Films 511 (2006) 634.
[27] E. Stathatos, V. Jovanovski, B. Orel, I. Jerman, P. Lianos, J. Phys. Chem. C 111 (2007) 6528.
[28] E. Stathatos, P. Lianos, Adv. Mater. 19 (2007) 3338.
[29] M. Antoniadou, P. Lianos, Eur. Phys. J. Appl. Phys. 51 (2010) 33211.
[30] E. Stathatos, P. Lianos, U.L. Stangar, B. Orel, P. Judeinstein, Langmuir 16 (2000) 8672.
[31] S. Ito, P. Chen, P. Comte, M.K. Nazeeruddin, P. Liska, P. Pechy, M. Gratzel, Prog. Photovolt.: Res. Appl. 15 (2007) 603.
[32] N. Papageorgiou, W.F. Maier, M. Gratzel, J. Electrochem. Soc. 144 (1997) 876M.
[33] T. Yohannes, O. Inganas, Sol. Energy Mater. Sol. Cells 51 (1998) 193.
[34] K.-C. Liu, M.A. Anderson, J. Electrochem. Soc. 143 (1996) 124.
[35] M. Zistler, P. Wachter, P. Wasserscheid, D. Gerhard, A. Hinsch, R. Sastawan, H.J. Gores, Electrochim. Acta 52 (2006) 161.
[36] F. Malara, M. Manca, L. De Marco, P. Pareo, G. Gigli, ACS Appl. Mater. Interfaces 3 (2011) 3625.
[37] M. Wu, X. Lin, L. Wang, W. Guo, Y. Wang, J. Xiao, A. Hagfeldt, T. Ma, J. Phys. Chem. C (2011), doi:10.1021/jp205886d.
[38] M.A. Green, K. Emery, Y. Hishikawa, W. Warta, Prog. Photovolt.: Res. Appl. 19 (2011) 84.